

Article

Anti-Metastatic Activity of Tagitinin C from *Tithonia diversifolia* in a Xenograft Mouse Model of Hepatocellular Carcinoma

Chuan-Yi Lin ^{1,2}, May-Hua Liao ³, Chi-Yu Yang ⁴, Chao-Kai Chang ^{5,6}, Shih-Mei Hsu ^{1,7}, Chi-Long Juang ¹ and Hsiao-Chuan Wen ^{8,*}

- ¹ Department of Medical Imaging and Radiological Technology, Yuanpei University of Medical Technology, Hsinchu 30015, Taiwan
 - ² Taiwan Instrument Research Institute, National Applied Research Laboratories, Hsinchu 300092, Taiwan
 - ³ Department of Nursing, Yuanpei University of Medical Technology, Hsinchu 30015, Taiwan
 - ⁴ Animal Technology Laboratories, Agricultural Technology Research Institute, Miaoli 35053, Taiwan
 - ⁵ Taipei Nobel Eye Institute, Taipei 100, Taiwan
 - ⁶ Department of Optometry, Yuanpei University of Medical Technology, Hsinchu 30015, Taiwan
 - ⁷ Department of Radiology, Mackay Memorial Hospital, Hsinchu 30071, Taiwan
 - ⁸ Department of Pet Healthcare, Yuanpei University of Medical Technology, Hsinchu 30015, Taiwan
- * Correspondence: sjwen@mail.ypu.edu.tw

Abstract: Sesquiterpenoid tagitinin C, present in *Tithonia diversifolia* leaves, has been known to have anti-hepatoma properties. Therefore, we investigated the anti-metastatic potential of tagitinin C in xenograft models of hepatocellular carcinoma (HCC). We isolated tagitinin C from a methanolic extract of the leaves of *T. diversifolia*. HepG-2 and Huh 7 hepatoma cells were treated with tagitinin C, and cell viability, migration, and matrix metalloproteinase (MMP) activity were assessed using the 3-(4,5-dimethylthiazol-2-yl)-2,5-diphenyltetrazolium bromide assay, scratch migration assay, and MMP activity assay, respectively. We used magnetic resonance spectroscopy to determine the tumorigenicity of xenografts inoculated with Hep-G2 and Huh 7 cells. Tagitinin C was cytotoxic against Hep-G2 and Huh 7 cells, with IC₅₀ values of 2.0 ± 0.1 µg/mL and 1.2 ± 0.1 µg/mL, respectively, and it showed an anti-metastatic effect in vitro. Additionally, MRS assays revealed that tagitinin C (15 g/mouse/day) reduced the tumorigenicity of Hep-G2 and Huh 7 cell xenografts. Tagitinin C demonstrated significant antitumor and anti-metastatic activity in the two human hepatoma cell lines. Tagitinin C might be used as an alternative or auxiliary therapy for the treatment of HCC, and its effect should be further investigated in clinical settings.

Keywords: tagitinin C; hepatocellular carcinoma; metastasis; *Tithonia diversifolia*; cancer; xenograft model



Citation: Lin, C.-Y.; Liao, M.-H.; Yang, C.-Y.; Chang, C.-K.; Hsu, S.-M.; Juang, C.-L.; Wen, H.-C. Anti-Metastatic Activity of Tagitinin C from *Tithonia diversifolia* in a Xenograft Mouse Model of Hepatocellular Carcinoma. *Livers* **2022**, *2*, 400–411. <https://doi.org/10.3390/livers2040030>

Academic Editor: Ralf Weiskirchen

Received: 5 October 2022

Accepted: 24 November 2022

Published: 1 December 2022

Publisher's Note: MDPI stays neutral with regard to jurisdictional claims in published maps and institutional affiliations.



Copyright: © 2022 by the authors. Licensee MDPI, Basel, Switzerland. This article is an open access article distributed under the terms and conditions of the Creative Commons Attribution (CC BY) license (<https://creativecommons.org/licenses/by/4.0/>).

1. Introduction

Among malignant cancers, hepatocellular carcinoma (HCC) is the third largest cause of cancer mortality worldwide [1] and the leading cause of cancer-related deaths in Taiwan [2]. The most common cause of death in patients with cancer is metastasis [3]. Therefore, controlling metastasis and understanding the processes underlying metastatic progression are essential for treating metastasis and cancer. Over the recent decades, anti-metastatic drugs have increasingly become the focus of research. Identification of novel anti-cancer agents is essential for overcoming the pitfalls of current treatment regimens, such as frequent recurrence and resistance to existing treatments.

The extracts of the stem and aerial parts of the plant *Tithonia diversifolia* have shown anti-inflammatory and liver-protective effects against carrageenan-induced paw edema and acute carbon tetrachloride-induced hepatic damage in rats [4]. *T. diversifolia* extracts, which contain tagitinin C, a major sesquiterpenoid, have been identified as potential therapeutic agents against cancer [5–7]. According to our recent study, there are several mechanisms

underlying the anti-hepatoma properties of *T. diversifolia* extracts [8]. In light of these findings, herein we aim to investigate the anti-metastatic effects of tagitinin C against human hepatoma in vitro and in vivo.

The movement of neoplastic cells is not a random process and is modulated by several molecular and cellular processes. Extracellular proteinases cleave matrix metalloproteinases (MMPs) into active proproteins when they are secreted. MMPs affect several aspects of cell function by cleaving the extracellular matrix and regulating the bioavailability of key factors involved in cell adhesion and migration [9,10]. MMP2 and MMP9 have previously been suggested as indicators of loss of tissue organization in malignant transformation [11]. MMP2 is also known as 72 kDa type IV collagenase or gelatinase A, whereas MMP9 is also known as 92 kDa type IV collagenase, 92 kDa gelatinase, or gelatinase B. Proteins of the MMP family (including MMP2 and MMP9) are involved in the breakdown of extracellular matrix under normal physiological conditions, such as during embryonic development and tissue remodeling, as well as under disease conditions, such as during arthritis, intracerebral hemorrhage, and metastasis.

Xenograft models of human HCC exhibit diffuse, compact trabeculae with variable degrees of anaplasia, increased mitotic and metastatic activity, and irregular masses. Hence, tumor volume and solid mass are not the only ways to investigate the effect of anti-tumorigenic agents. Since cell membrane degradation results in the release of glycerophosphocholine by necrotic tumors, causing an increase in choline concentration [12–14], choline ^1H magnetic resonance spectroscopy (MRS) is used to evaluate the prognosis of various tumor types. Non-invasive measurements of metabolites can be performed repeatedly in living animals and patients using in vivo MRS. Therefore, we used MRS to assess the anti-tumorigenic effects of tagitinin C on Hep-G2 and Huh 7 xenografts.

2. Methods

2.1. Plant Material and Tagitinin C Preparation

The leaves of *T. diversifolia* were collected in January 2020 in Hsin-Chu, Taiwan. A methanolic extract of the powdered leaves of the plant was prepared at 25 °C and concentrated under reduced pressure using a rotary vacuum evaporator (RV 3 V: IKA, Taiwan). Ethyl acetate (EtOAc)-partitioning of the methanolic extract was performed, yielding two subfractions: EtOAc-soluble and water-soluble. The EtOAc-soluble fraction was subjected to elution using hexane/EtOAc and EtOAc/methanol gradients to isolate tagitinin C. Next, the extract was analyzed by proton nuclear magnetic resonance (^1H NMR) as follows: in ^1H NMR (500 MHz, CDCl_3) δ : 6.89 (d, J = 17.0 Hz, ^1H , H-1), 6.27 (d, J = 1.1 Hz, ^1H , H α -13), 6.19 (d, J = 17.0 Hz, ^1H , H-2), 5.80 (dq, J = 8.8, 1.1 Hz, ^1H , H-5), 5.74 (d, J = 1.1 Hz, ^1H , H β -13), 5.37 (br. d, J = 8.8, ^1H), 5.82 (m, 1H, H-8), 3.50 (m, ^1H , H-7), 3.21 (s, ^1H , -OH), 2.41 (dd, J = 13.9, 6.3 Hz, ^1H , H α -9), 2.36 (seq, J = 6.9 Hz, ^1H , H -2'), 1.94 (dd, J = 13.9, 10.0 Hz, ^1H , H β -9), 1.88 (br. s, ^3H), 1.47 (s, ^3H , H-14), 0.99 (d, J = 6.9 Hz, ^3H , H-3'), 0.97 (d, J = 6.9 Hz, ^3H , H-4'). The HPLC analysis certified the content of tagitinin C, the major sesquiterpenoid in the *Tithonia diversifolia* methanolic extract, at 1.45% and the purity at more than 95%. A stock solution of tagitinin C was prepared by pre-dissolving it in dimethyl sulfoxide (DMSO) to a final concentration of 100 $\mu\text{g}/\text{mL}$ before subsequent dilution for cell culture.

2.2. Cell Culture

Human hepatoma cell lines, Hep-G2 and Huh 7, and mouse liver cell line, Clone 9, were incubated separately in Dulbecco's Modified Eagle's Medium (Life Technologies, Grand Island, NY, USA), supplemented with 10% fetal calf serum, 2 mM glutamine, 100 U/mL penicillin, 100 mg/mL streptomycin sulfate, 0.1 mM non-essential amino acids, and 1 mM sodium pyruvate at 37 °C. Huh 7, Clone 9, and Hep-G2 cells were cultured in 6 cm culture dishes and treated with tagitinin C (1.25, 2.5, and 5 mg/mL) or 0.1% DMSO (negative control).

2.3. Cell Viability Assay

Trypan blue assay and the 3-(4,5-dimethylthiazol-2-yl)-2,5-diphenyltetrazolium bromide (MTT) spectrophotometric assay were used to determine cell viability. Cell reduction assays were used to determine IC₅₀ values. Cells were seeded at a concentration of 7×10^3 cells/mL in 96-well culture plates and allowed to adhere for 24 h. After adding tagitinin C, we incubated the plates for another 24 h. Next, the cells were washed with phosphate-buffered saline, and MTT (1 mg/mL)-containing medium, free of fetal bovine serum, was added to the cells, followed by incubation for 4 h at 37 °C. Subsequently, the medium was discarded, and the resultant insoluble formazan blue was dissolved in DMSO. The optical density was measured at 540 nm using a microplate reader (Multiskan™ FC; Thermo Fisher Scientific, Waltham, MA, USA).

2.4. Cell Migration Assay

Cell migration of Hep-G2 and Huh 7 cells was assessed using a wound healing assay. First, a wound was created by scratching a monolayer of cells. Next, the cells were incubated in a medium containing 0.1% DMSO or 1.25, 2.5, or 5 g/mL tagitinin C. Wounds were photographed at 0 and 24 h after scratching. The wound closure distance was analyzed using AxioVision software (Carl Zeiss, Braunschweig, Germany), and the difference in wound closure distance between 0 and 24 h was determined.

2.5. MMP2 and MMP9 Activity Assay

Proteins in cell lysates (50 µg) were separated by collagen zymography under non-reducing conditions with gelatin (Sigma-Aldrich, St. Louis, MO, USA) at a final concentration of 0.5 mg/mL in 9% total acrylamide gel. Laemmli buffer was used, and electrophoresis was conducted for 1 h at 4 °C. After washing the gel with 2.5% Triton X-100, we incubated the gels in 50 mM Tris-HCl, 10 mM CaCl₂, and 50 mM NaCl (pH 7.6) for 60 min. Next, gels were stained with 0.25% Coomassie brilliant blue R-250 (Bio-Rad, Hercules, CA, USA) in 40% methanol and 10% acetic acid, and then destained with 40% methanol and 10% acetic acid. Protease activity was visualized as clear (unstained) bands. A densitometer equipped with IMAGEQUANT® software (Molecular Dynamics, Sunnyvale, CA, USA) was used to quantify the bands.

2.6. Tumorigenicity in Nude Mice

The Experimental Animal Center of Taiwan University (Taipei, Taiwan) provided five-week-old female BALB/c nude mice (16–18 g). The mice were randomly divided into four groups (n = 5 per group) for the tumorigenicity test. Untreated Hep-G2 or Huh 7 cells (1.5×10^7) were injected subcutaneously into the dorsum of each mouse. Two days after inoculating the mice with hepatoma cells, tagitinin C (15 mg/mouse/day) or 0.075% DMSO were administered intraperitoneally as described previously [15]. After 3–4 days of drug administration, mice were scanned using MRI and MRS. After 25 days, mice were anesthetized by a sodium pentobarbital overdose and sacrificed. Blood samples were obtained from the left ventricle, and serum was collected by centrifugation at $1500 \times g$ for 10 min at 4 °C and stored at −80 °C until further use. Yuanpei University's Experimental Animal Ethical Committee approved all experimental protocols in accordance with the National Institutes of Health Guide for the Care and Use of Laboratory Animals.

2.7. In Vivo MR Analysis

In vivo MRI and MRS were performed using a 1.5-Tesla MR system (Siemens, Erlangen, Germany). Zoletil 50® (50 mg/kg) was used to anesthetize the animals (n = 5 per time course). The animals were placed on a warm waterbed to maintain their body temperature at 36 °C. Prior to spectroscopy acquisition, we performed conventional T2-weighted MRI. To acquire chemical shift imaging (CSI) data, we used a $30 \times 30 \times 10$ mm³ voxel (divided into eight columns and eight rows) and five averages. A point-resolved spectroscopic sequence was used to obtain all spectra (repetition time/echo time of 1500/135 ms). Before

each acquisition, field homogeneity was automatically adjusted over the selected volume of interest. Each scan protocol included automatic shimming and water suppression. Each CSI acquisition took approximately 8 min and 20 s. Post-processing of the data included phase and baseline corrections. A peak area was measured at the cancer-cell inoculation points of choline and creatine (3.2 ppm and 3.0 ppm, respectively). Choline/creatine ratios were calculated based on CSI results; creatine was used as an internal standard.

2.8. Serologic Tests

Glutamate pyruvate transaminase (GPT) was quantified using a chemical analyzer (Hitachi 7170; Hitachi Hi-Tech, Tokyo, Japan). The cobas e411 analyzer (Roche, Basel, Switzerland) with electrochemiluminescence was used to determine serum alpha-fetoprotein (AFP) concentrations.

2.9. Statistical Analysis

The data from three independent experiments are presented as the mean \pm standard deviation. One-way analysis of variance and Duncan's multiple range test were used to evaluate differences between groups. Student's *t*-test was used to compare the control and treatment groups. All data were analyzed using the Statistical Analysis Software (SAS Institute, Cary, NC, USA). Differences were considered statistically significant at $p < 0.05$.

3. Results

The in vitro activity of tagitinin C was previously evaluated in a normal cell line (Clone 9) and hepatoma cell lines (Hep-G2 and Huh 7). Table 1 shows the IC₅₀ values for tagitinin C in the three cell lines. The MTT assay (Figure 1), cell cycle phase arrest (Table 2), and flow cytometric analyses (Figure 2) in Hep-G2 and Huh 7 cells revealed that tagitinin C reduced cell viability in a dose-dependent manner. In hepatoma cells, treatment with tagitinin C significantly elevated the levels of cleaved caspase 3 and caspase 8, indicating DNA damage and apoptosis.

Table 1. IC₅₀ values for tagitinin C in normal cell lines (Clone 9) and hepatoma cell lines (Hep-G2 and Huh 7) after 24 h of treatment.

Cells	IC ₅₀ (mg/mL)
Clone 9	8.6 \pm 6.0
Hep-G2	2.0 \pm 0.1
Huh 7	1.2 \pm 0.1

Table 2. Flow-cytometric analysis of the effects of tagitinin C on the Huh 7 cell cycle after 24 h of treatment. Huh 7 cells (8×10^5 cells/mL) treated with or without tagitinin C for 24 h were harvested and fixed with 1 mL of ice-cold 70% ethanol at 4 °C for 2 h. The proportion of cell cycle phases was analyzed using fluorescence-activated cell sorting flow cytometry (BD FACSCalibur™ Flow Cytometer; BD Biosciences, San Jose, CA, USA). ** $p < 0.01$ vs. control, *** $p < 0.001$ vs. control. The groups were compared using the Student's *t*-test.

% of Total Cells	Sub G1	G1	G2/M	S
Control	1.14 \pm 0.19	57.64 \pm 1.36	28.83 \pm 0.63	10.56 \pm 0.96
1.25 μ g/mL	46.48 \pm 4.89 ***	31.60 \pm 2.21 ***	5.34 \pm 0.71 ***	8.71 \pm 0.75 **
2.5 μ g/mL	93.64 \pm 1.10 ***	4.94 \pm 0.88 ***	0.26 \pm 0.08 ***	1.03 \pm 0.30 ***
5 μ g/mL	89.88 \pm 4.57 ***	8.48 \pm 3.97 ***	0.20 \pm 0.72 ***	1.33 \pm 0.64 ***

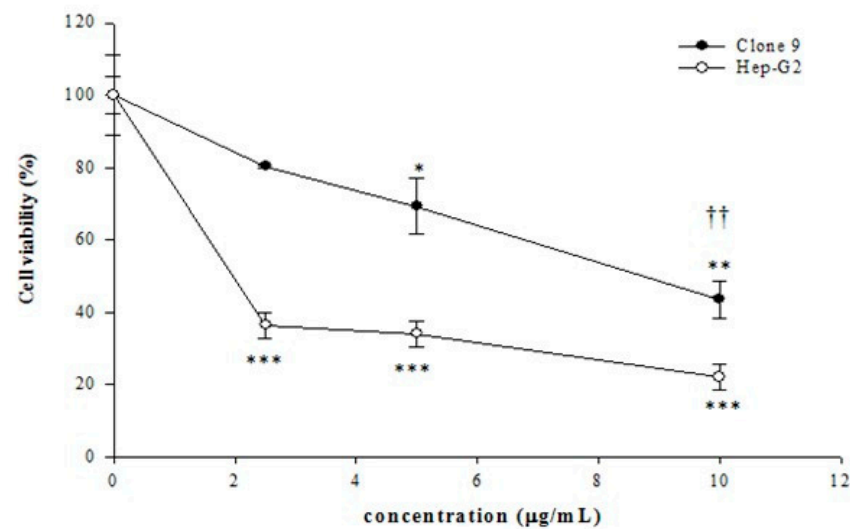


Figure 1. Cytotoxic effects of tagitinin C at various concentrations on Clone 9 (normal) and Huh 7 (hepatoma) cells. The data represent the mean \pm standard deviation of three independent experiments. (* $p < 0.05$ vs. control, ** $p < 0.01$ vs. control, *** $p < 0.001$ vs. control, ++ $p < 0.01$ Clone 9 vs. Huh 7 cells).

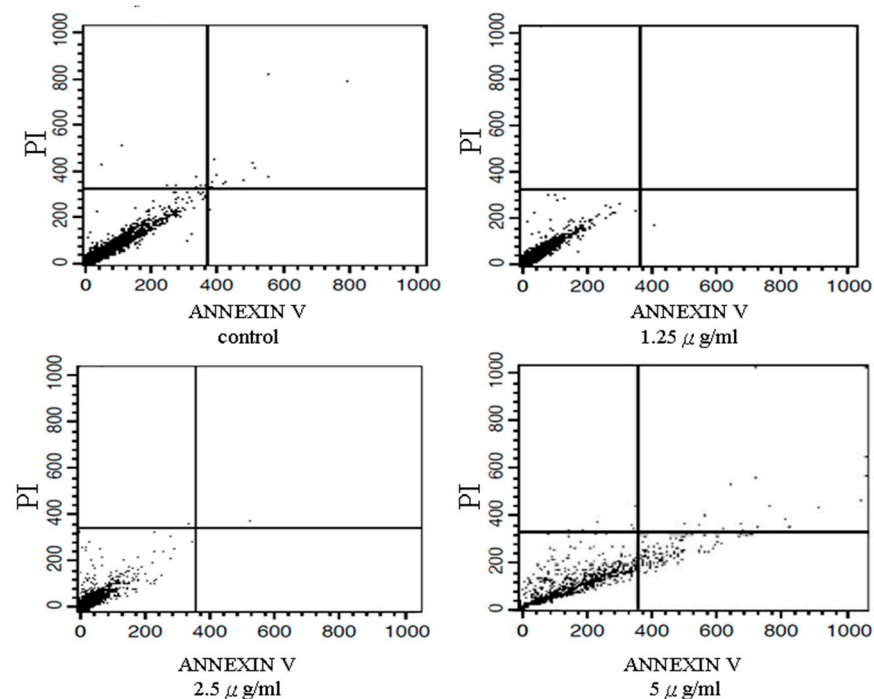


Figure 2. Results of flow cytometric analyses. Effects of tagitinin C on apoptosis in a hepatoma cell line. Huh 7 cells (8×10^5 cells/mL), treated with or without tagitinin C for 24 h, were harvested and fixed with 1 mL of ice-cold 70% ethanol at 4 °C for 2 h. Annexin V is a phospholipid-binding protein that has affinity for phosphatidylserine (PS) and is used to analyze apoptotic activity. Test cells were stained using an Annexin V-FITC assay kit (Dojindo, FoliBio Technology Co., Ltd., Taipei, Taiwan) for 15 min and then treated with propidium iodide (PI) for 30 min in the dark. The apoptotic cell distribution was analyzed by fluorescence-activated cell sorting flow cytometry (BD FACSCalibur™ Flow Cytometer; BD Biosciences).

Tagitinin C significantly reduced the cell migration of Hep-G2 ($p < 0.05$; Figure 3A) and Huh 7 ($p < 0.05$; Figure 3B) cells. Moreover, tagitinin C significantly inhibited MMP2

and MMP9 activity, suggesting that it may exhibit an anti-metastatic effect via MMP2 and MMP9 (Figure 4).

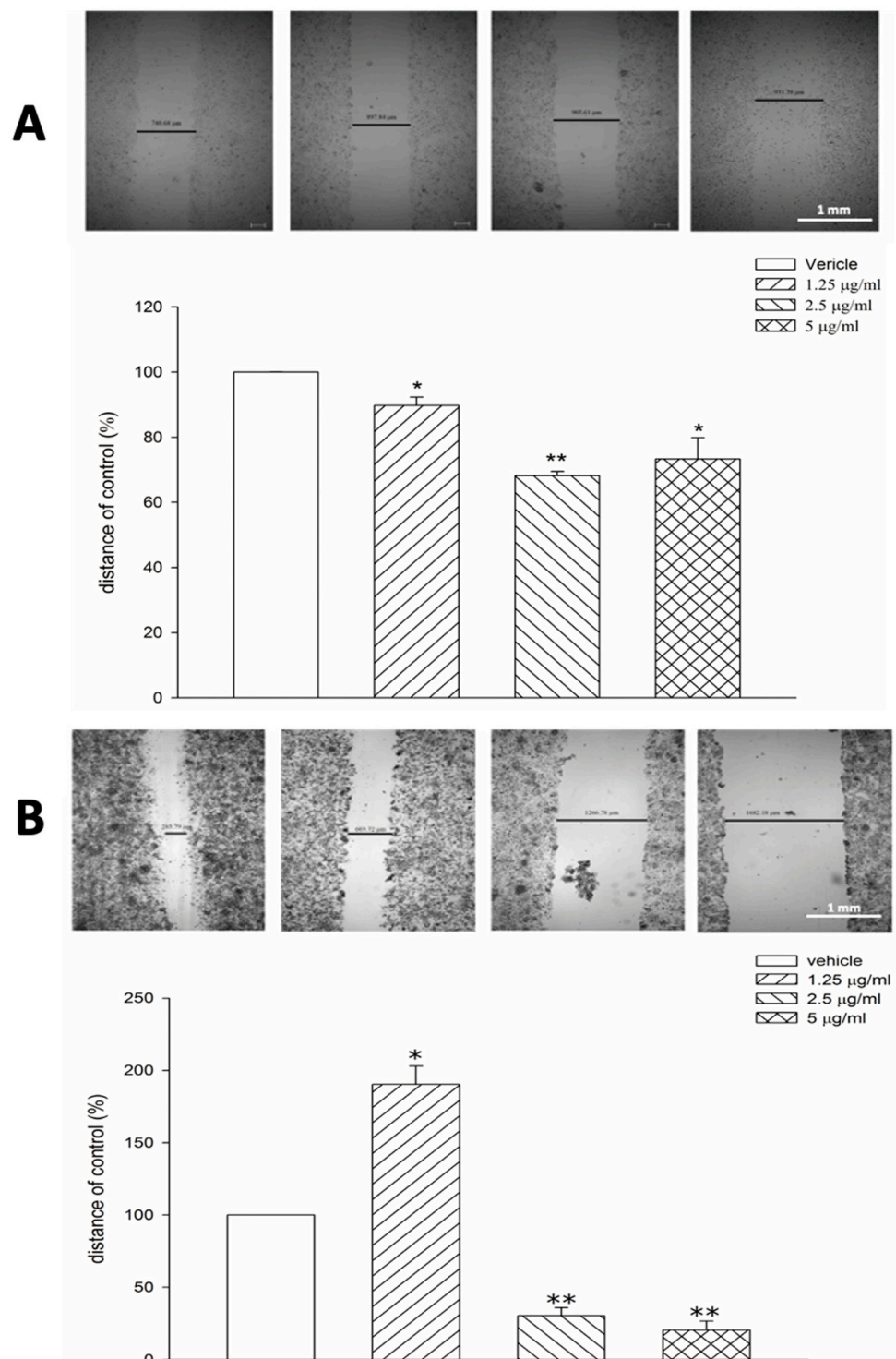


Figure 3. Tagitinin C inhibits cell migration of Hep-G2 and Huh 7 cells. **(A)** Scratch migration assay of Hep-G2 cells (control or tagitinin C-treated cells). **(B)** Scratch migration assay of Huh 7 cells (control or tagitinin C-treated cells). * $p < 0.05$ vs. control, ** $p < 0.01$ vs. control.

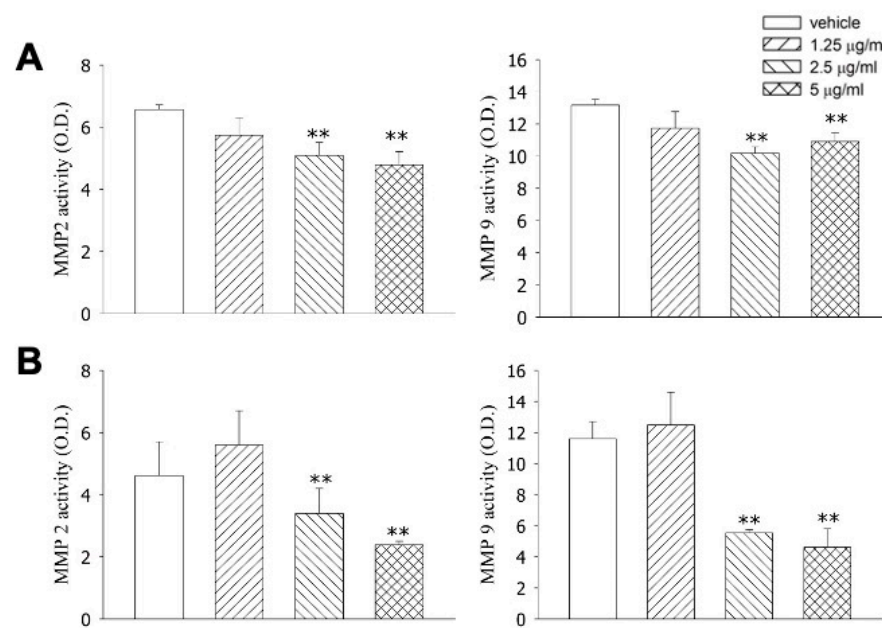


Figure 4. Effects of tagitinin C on MMP2 and MMP9 activity based on a collagen zymography assay. (A) Effects of tagitinin C on MMP2 and MMP9 activity in Hep-G2 cells. (B) Effects of tagitinin C on MMP2 and MMP9 activity in Huh 7 cells. ** $p < 0.01$ vs. control.

Next, *in vivo* effects of tagitinin C were evaluated using MRS. The control and experimental groups showed variable degrees of anaplasia, increased mitotic and metastatic activity, and irregular masses on macroscopic examination. As revealed by the MR assay, tumor cells spread throughout the abdomen and metastasized to several organs in the xenografted mice. Since evaluation of the significantly reduced hepatoma mass compared to that in the control mice was not possible (Figure 5), we acquired the multi-voxel spectra of the hepatoma after 25 days of inoculation with Hep-G2 cells. Based on the MRS of voxel 1, Hep-G2 inoculated voxel 1 had low choline levels (shown in the MRS of voxel 1). Voxel 2 had the highest levels of choline in the same cross-section. Hep-G2 cells migrated from voxel 1 to voxel 2, as indicated by high choline levels. Creatine was used as an internal standard.

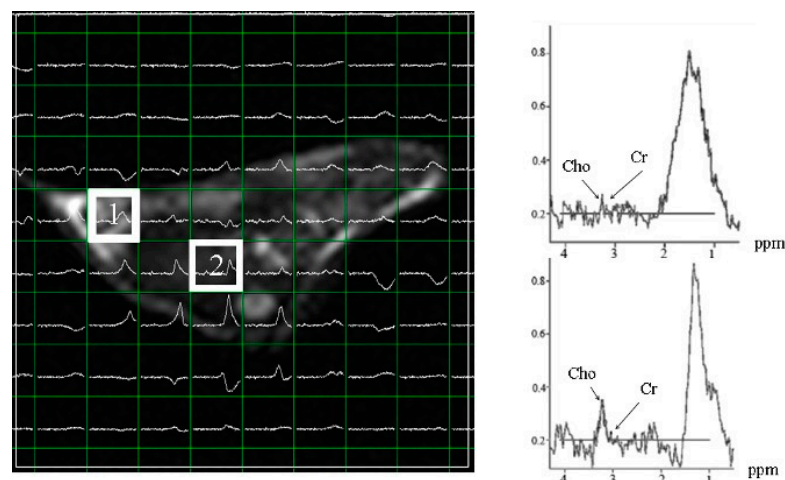


Figure 5. Multi-voxel spectra of hepatoma in subcutaneous Hep-G2-xenografted mice after 25 days of inoculation. Voxel 1 shows the inoculation point of Hep-G2. Voxel 2 shows the maximum choline levels, indicating that Hep-G2 cells migrated from voxel 1 to voxel 2. Cho: choline; Cr: creatine.

Subcutaneous Hep-G2- and Huh 7-xenografted mice were examined for multi-voxel hepatoma spectra at 25 days post-inoculation (Figure 6A,C). Hep-G2 xenografts showed the maximum level of choline/creatine at a different site from the inoculation point (Figure 6B), whereas the maximum choline/creatine level was observed near the inoculation point in Huh 7 xenografts (Figure 6D). These results suggest a greater capability of Hep-G2 cells to metastasize than that of Huh 7 cells.

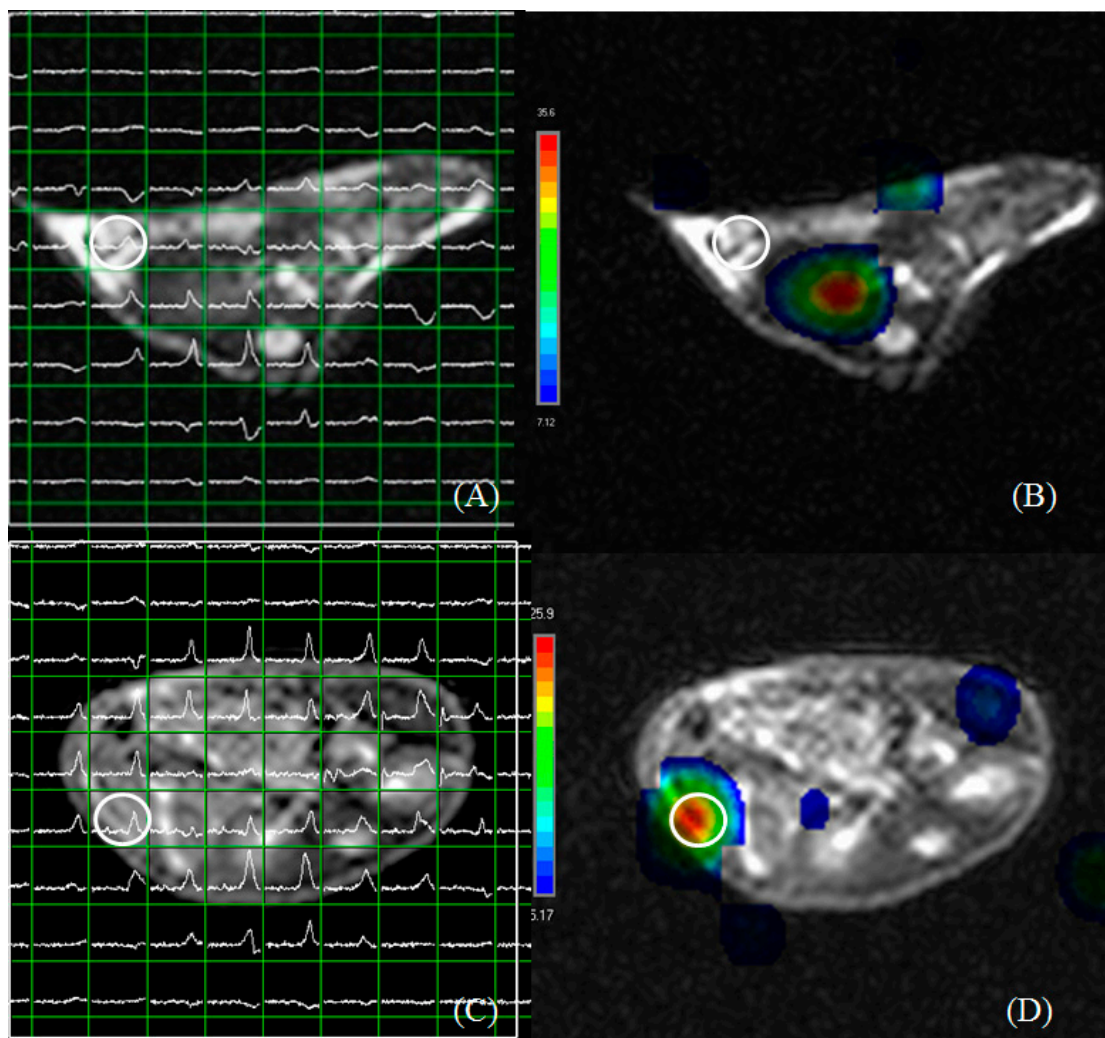


Figure 6. Multi voxel spectra of hepatoma in subcutaneous Hep-G2- (A,B) and Huh 7- (C,D) xenografted mice at 25 days post-inoculation. (A) The choline/creatine level at the inoculated point in (B). (C) The choline/creatine level at the inoculation point in (D). The maximum choline/creatine level was detected at some distance from the inoculation point in Hep-G2-xenografted mice. The maximum choline/creatine level was near the inoculation point in Huh 7-xenografted mice. Circles indicate the point of inoculation.

Xenografted mice derived from two hepatoma cell lines showed minimal choline/creatine levels at the time of inoculation compared to those in the vehicle group. However, choline levels were higher in regions distant from those at the site of inoculation (Table 3), indicating that the two cancer cell lines metastasized to other parts after approximately 5–25 days of inoculation. Further, tagitinin C treatment (15 g/mouse/day) for 15–25 days reduced the tumorigenicity of xenografts derived from the two cell lines.

Table 3. Effects of tagitinin C on alpha-fetoprotein (AFP) and glutamate pyruvate transaminase (GPT) and choline/creatine ratio according to chemical shift imaging of two hepatocellular carcinoma xenograft lines. Representative AFP and GPT values from tagitinin C (15 µg/mouse/day)-treated and vehicle (0.075% DMSO)-treated groups. The Cho/Cr ratio at maximum represents the reading for the pixel with the maximum ratio on the whole slice. All mice were euthanized after the MR assay. ^a $p < 0.05$ when compared to vehicles in the same group. ^b $p < 0.05$ compared with experimental values after treatment for 25 days. ^c $p < 0.05$ when compared to the vehicle after 15 days of treatment. Differences between groups were compared using the Student's *t*-test. Tc: tagitinin C; Cho/Cr: choline/creatine.

Cell	Day	Group	AFP (ng/mL)	GPT (U/L)	Cho/Cr at Inoculated Pixel	Cho/Cr at Maximum
Hep-G2	5	Vehicle	<0.61	136.0 ± 46.6	0.93 ± 0.93	55.81 ± 16.02
		Tc	<0.61	29.3 ± 5.9	11.52 ± 4.80 ^a	31.83 ± 8.12 ^a
	15	Vehicle	890.0 ± 191.7	28.4 ± 2.5	0.00 ± 0.00	72.40 ± 9.70
		Tc	961.8 ± 185.3	68.8 ± 38.1	6.53 ± 3.83 ^a	29.32 ± 6.30 ^a
	25	Vehicle	>12,100	362.4 ± 124.00	0.15 ± 0.15	34.49 ± 5.52 ^b
		Tc	>12,100	74.3 ± 27.00 ^c	1.87 ± 0.87 ^a	13.19 ± 2.52 ^c
Huh 7	5	Vehicle	<0.61	125.05 ± 61.52	9.72 ± 6.63	42.75 ± 17.79
		Tc	<0.61	195.00 ± 79.80	11.10 ± 2.02	29.28 ± 7.66
	15	Vehicle	<0.61	49.66 ± 7.28	6.16 ± 2.41	47.34 ± 7.92 ^b
		Tc	<0.61	86.28 ± 25.10 ^b	10.31 ± 3.67	22.62 ± 6.04 ^a
	25	Vehicle	>12,100	32.3 ± 3.55	0.54 ± 0.38	67.85 ± 13.09 ^c
		Tc	>12,100	279 ± 208	3.90 ± 2.95	14.37 ± 4.46 ^a

4. Discussion

Tagitinin C extracted from *T. diversifolia* leaves inhibited the growth of hepatoma cells both in vitro and in vivo, and this process was associated with apoptosis [16]. We treated cells and xenografted mice with tagitinin C to test its anti-metastatic effects on hepatoma cell lines in vitro and in vivo in a xenograft mouse model.

Biological activities of chemical compounds present in natural plant extracts make them an important source of anti-tumor drugs; furthermore, natural plant extracts are generally less toxic and have fewer side effects than chemically synthesized drugs. In recent years, there has been an increased research focus on natural plant extracts and their functional mechanisms. In the present study, we showed that tagitinin C inhibited the proliferation of Hep-G2 and Huh 7 cells, with IC₅₀ values of 2.0 ± 0.1 µg/mL and 1.2 ± 0.1 µg/mL, respectively. In Hep-G2 and Huh 7 cells, tagitinin C-induced anti-metastatic and anti-angiogenic effects have been observed; furthermore, the antiproliferative effect of tagitinin C through cell cycle arrest has been described previously in cancer cells [17]. Inhibition of metastasis by tagitinine C may be related to fibroblast growth factors, vascular endothelial growth factors, or platelet-derived growth factors, either alone or in conjunction with other signaling pathways.

In various studies evaluating the anticancer effects of tagitinin C, it can be speculated that tagitinin C isolates have cytotoxic abilities through various pathways. For example, tagitinin C can increase the expression of the p53 protein in HeLa cells, enhancing the apoptotic capacity [18]. Another study showed that tagitinin C isolate could reduce VEGF expression in colon cancer cells [19]. The mechanism of VEGF expression inhibition by tagitinin C isolates is suspected to be caused by the NF-κB transcriptional barrier through the alkylation of the cystine residue (Cys 38) p. 56 [20,21].

Studies have also shown that tagitinin C increases cellular reactive oxygen species (ROS), lipid peroxidation, malondialdehyde (MDA) content, and the labile iron pool [22]. In contrast, tagitinin C treatment has been shown to decrease glutathione (GSH) levels in HCT116 cells [23]. The enzyme heme oxygenase 1 (HO-1) metabolizes heme into pro-oxidative ferrous iron, carbon monoxide, and the antioxidant biliverdin in the endoplasmic reticulum (ER). A study revealed that HO-1 has a cytoprotective effect in various stress-

related conditions [24]. Moreover, HO-1 is an essential positive regulator of ferroptosis, making it a potential mediator of harmful outcomes [25]. HO-1 expression was induced by Betulaceae extract in human colon cancer cells [26]. In addition to accelerating erastin-mediated ferroptosis in HT-1080 fibrosarcoma cells, HO-1 facilitates BAY 11-7085-induced ferroptosis in breast cancer cells [27,28]. Heme degradation and Nrf2-mediated HO-1 upregulation are both involved in doxorubicin-induced cardiomyocyte ferroptosis [29]. Withaferin A, a natural ferroptide, promoted ferroptosis in neuroblastoma by inducing iron accumulation and ROS production [30]. According to these findings, HO-1 regulates cellular iron levels and ROS levels to cause ferroptotic cell death. Iron and ROS homeostasis and ferroptosis induction are regulated by HO-1, which can have either cytoprotective or harmful effects. The Nrf2-HO-1 signaling pathway is also activated by tagitinin C, causing high HO-1 expression within 6 h and resulting in cellular iron accumulation and ferroptosis [23].

ER stress is also associated with ROS production [31,32]. Protein synthesis, folding, secretion, and post-translational modifications are regulated by the ER. ER stress occurs when misfolded proteins accumulate in the ER in response to micro-environmental stimuli [33]. Cells respond to ER stress by activating three distinct signaling pathways, including the protein kinase RNA-like endoplasmic reticulum kinase (PERK) pathway, which initiates the unfolded protein response (UPR). PERK is phosphorylated and activated by BiP [32,33], followed by the phosphorylation of Nrf2, a transcription factor. The latter dissociates from the Nrf2/Keap1 complex in the cytoplasm and then translocates to the nucleus, where Nrf2 interacts with anti-oxidant response elements and transactivates various genes, including HO-1, GCLM, SLC7A11, GCLC, FTH1, ATF6, NQO1, GAPDH, ATF3, and Nrf2 itself [34]. Both ER stress and the UPR are involved in cancer development and play a critical role in ferroptosis [35,36]. A previous study has demonstrated activation of the PERK pathway by tagitinin C. Furthermore, the Nrf2-HO-1 signaling pathway was activated by ER stress and PERK inhibitors [23]. Along with ferroptosis, apoptosis can be induced by tagitinin C at later stages. Lipid peroxidation is the hallmark of ferroptosis. In addition to propagating lipid peroxidative chains, excessive ROS attacks biofilms and initiates different forms of cell death [37]. Ferroptosis and apoptosis are cross-reliant on ER stress [38].

In this study, clinically relevant MR techniques were applied. For example, MRS was used instead of conventional MR techniques. By sampling biochemical information from both tumor and normal tissue samples, ¹H MRS can complement MR. Hepatoma tumors greater than 12 mm in diameter showed an increased choline signal, consistent with the results of previous reports, suggesting that choline level reflects tumor cell proliferation and malignancy grade [39,40]. Therefore, choline signals can be used to determine the response of tumors to anti-tumor treatments. The present study had a few limitations. Respiratory movement during abdominal MR imaging might have caused poor image quality and variations in measurements because breath-holding or respiratory gating techniques are difficult to apply in mice. First, we anesthetized the mice using sodium pentobarbital, and then we scanned them with MR and obtained their blood samples for serological testing. We obtained repeated and statistically significant measurements despite this potential limitation. MRS with clinical 1.5-T MR imaging was successfully used to investigate a liver tumor model. Therefore, this technique could be used to perform preclinical evaluations of new therapeutics.

5. Conclusions

The present study is the first to investigate the anti-metastatic properties of tagitinin C. Tagitinin C inhibits the proliferation, migration, and metastasis of HCC cells, both *in vitro* and *in vivo*.

Author Contributions: Data collection, analysis, and manuscript—draft preparation: C.-Y.L.; experimental design and analysis: M.-H.L., C.-Y.Y., C.-K.C., S.-M.H. and C.-L.J.; study conceptualization, supervision, and manuscript revision: H.-C.W. All authors have read and agreed to the published version of the manuscript.

Funding: The study was funded by grants from the Ministry of Science and Technology (MOST 109-2637-B-264-001), NSC 97-2113-M-264-001, NSC 98-2622-M-264-002-CC3 and industry-academia cooperation at Yuanpei University (109-COMP6011-04) for research.

Institutional Review Board Statement: Yuanpei University's Experimental Animal Ethical Committee approved all experimental protocols in accordance with the National Institutes of Health Guide for the Care and Use of Laboratory Animals.

Informed Consent Statement: Not applicable.

Data Availability Statement: The datasets used and/or analyzed in the current study are available from the corresponding author on reasonable request.

Conflicts of Interest: The authors declare no conflict of interest.

References

1. Jemal, A.; Murray, T.; Ward, E.; Samuels, A.; Tiwari, R.C.; Ghafoor, A.; Feuer, E.J.; Thun, M.J. Cancer Statistics, 2005. *CA Cancer J. Clin.* **2005**, *55*, 10–30. [\[CrossRef\]](#) [\[PubMed\]](#)
2. Hsiao, A.-J.; Chen, L.-H.; Lu, T.-H. Ten leading causes of death in Taiwan: A comparison of two grouping lists. *J. Formos Med. Assoc.* **2015**, *114*, 679–680. [\[CrossRef\]](#) [\[PubMed\]](#)
3. Weinberg, R.A.; Weinberg, R.A. *The Biology of Cancer*; WW Norton & Company: New York, NY, USA, 2006.
4. Lin, C.C.; Lin, M.L.; Lin, J.M. The antiinflammatory and liver protective effect of *Tithonia diversifolia* (Hemsl.) gray and *Dicliptera chinensis* Juss. Extracts in rats. *Phytother. Res.* **1993**, *7*, 305–309. [\[CrossRef\]](#)
5. Kuroda, M.; Yokosuka, A.; Kobayashi, R.; Jitsuno, M.; Kando, H.; Nosaka, K.; Ishii, H.; Yamori, T.; Mimaki, Y. Sesquiterpenoids and flavonoids from the aerial parts of *Tithonia diversifolia* and their cytotoxic activity. *Chem. Pharm. Bull.* **2007**, *55*, 1240–1244. [\[CrossRef\]](#) [\[PubMed\]](#)
6. Liao, M.-H.; Lin, W.-C.; Wen, H.-C.; Pu, H.-F. *Tithonia diversifolia* and its main active component tagitin C induce survivin inhibition and G2/M arrest in human malignant glioblastoma cells. *Fitoterapia* **2011**, *82*, 331–341. [\[CrossRef\]](#)
7. Lee, M.-Y.; Liao, M.-H.; Tsai, Y.-N.; Chiu, K.-H.; Wen, H.-C. Identification and anti-human glioblastoma activity of tagitin C from *Tithonia diversifolia* methanolic extract. *J. Agric. Food Chem.* **2011**, *59*, 2347–2355. [\[CrossRef\]](#) [\[PubMed\]](#)
8. Liao, M.H.; Tsai, Y.N.; Yang, C.Y.; Juang, C.L.; Lee, M.Y.; Chang, L.H.; Wen, H.C. Anti-human hepatoma Hep-G2 proliferative, apoptotic, and antimutagenic activity of tagitin C from *Tithonia diversifolia* leaves. *J. Nat. Med.* **2013**, *67*, 98–106. [\[CrossRef\]](#)
9. Egeblad, M.; Werb, Z. New functions for the matrix metalloproteinases in cancer progression. *Nat. Rev. Cancer* **2002**, *2*, 161–174. [\[CrossRef\]](#)
10. Page-McCaw, A.; Ewald, A.J.; Werb, Z. Matrix metalloproteinases and the regulation of tissue remodelling. *Nat. Rev. Mol. Cell Biol.* **2007**, *8*, 221–233. [\[CrossRef\]](#)
11. Bissell, M.; Kenny, P.; Radisky, D. Microenvironmental regulators of tissue structure and function also regulate tumor induction and progression: The role of extracellular matrix and its degrading enzymes. In *Cold Spring Harbor Symposia on Quantitative Biology*; Cold Spring Harbor Laboratory Press: Cold Spring Harbor, NY, USA, 2005; pp. 343–356.
12. Bizzi, A.; Movsas, B.; Tedeschi, G.; Phillips, C.L.; Okunieff, P.; Alger, J.R.; Di Chiro, G. Response of non-Hodgkin lymphoma to radiation therapy: Early and long-term assessment with H-1 MR spectroscopic imaging. *Radiology* **1995**, *194*, 271–276. [\[CrossRef\]](#)
13. Schwarz, A.; Maisey, N.; Collins, D.; Cunningham, D.; Huddart, R.; Leach, M. Early in vivo detection of metabolic response: A pilot study of 1H MR spectroscopy in extracranial lymphoma and germ cell tumours. *Br. J. Radiol.* **2002**, *75*, 959–966. [\[CrossRef\]](#) [\[PubMed\]](#)
14. Radermacher, K.A.; Magat, J.; Bouzin, C.; Laurent, S.; Dresselaers, T.; Himmelreich, U.; Boutry, S.; Mahieu, I.; Vander Elst, L.; Feron, O. Multimodal assessment of early tumor response to chemotherapy: Comparison between diffusion-weighted MRI, 1H-MR spectroscopy of choline and USPIO particles targeted at cell death. *NMR Biomed.* **2012**, *25*, 514–522. [\[CrossRef\]](#) [\[PubMed\]](#)
15. Kaur, P.; Shukla, S.; Gupta, S. Plant flavonoid apigenin inactivates Akt to trigger apoptosis in human prostate cancer: An in vitro and in vivo study. *Carcinogenesis* **2008**, *29*, 2210–2217. [\[CrossRef\]](#)
16. Lu, M.R.; Huang, H.L.; Chiou, W.F.; Huang, R.L. Induction of Apoptosis by *Tithonia diversifolia* in Human Hepatoma Cells. *Pharmacogn Mag* **2017**, *13*, 702–706. [\[CrossRef\]](#)
17. Cragg, G.M.; Grothaus, P.G.; Newman, D.J. Impact of natural products on developing new anti-cancer agents. *Chem. Rev.* **2009**, *109*, 3012–3043. [\[CrossRef\]](#) [\[PubMed\]](#)
18. Mandela, W. Pengaruh Senyawa Isolat Aktif daun Kembang Bulan (*T. diversifolia*) Terhadap Ekspresi Protein p53 Pada Sel Hela Dengan Metode Immunohistokimia [Skripsi]; Fakultas Kedokteran Universitas Gadjah Mada: Yogyakarta, Indonesia, 2010.
19. Mh, H.R. Aktivitas Isolat Aktif Daun Kembang Bulan [*Tithonia diversifolia* (Hemsl.) a. Gray] Pada Siklus sel dan Angiogenesis sel Widr Secara In Vitro; Universitas Gadjah Mada: Yogyakarta, Indonesia, 2012.
20. Rüngeler, P.; Lyß, G.; Castro, V.; Mora, G.; Pahl, H.L.; Merfort, I. Study of three sesquiterpene lactones from *Tithonia diversifolia* on their anti-inflammatory activity using the transcription factor NF-κB and enzymes of the arachidonic acid pathway as targets. *Planta Med.* **1998**, *64*, 588–593. [\[CrossRef\]](#)

21. García, A.; Delgado, G. Constituents from *Tithonia diversifolia*: Stereochemical revision of 2 α -hydroxytirofendin. *J. Mex. Chem. Soc.* **2006**, *50*, 180–183.
22. Hassannia, B.; Vandenabeele, P.; Berghe, T.V. Targeting ferroptosis to iron out cancer. *Cancer Cell* **2019**, *35*, 830–849. [[CrossRef](#)]
23. Wei, R.; Zhao, Y.; Wang, J.; Yang, X.; Li, S.; Wang, Y.; Yang, X.; Fei, J.; Hao, X.; Zhao, Y.; et al. Tagitinin C induces ferroptosis through PERK-Nrf2-HO-1 signaling pathway in colorectal cancer cells. *Int. J. Biol. Sci.* **2021**, *17*, 2703–2717. [[CrossRef](#)]
24. Gottlieb, Y.; Truman, M.; Cohen, L.A.; Leichtmann-Bardoogo, Y.; Meyron-Holtz, E.G. Endoplasmic reticulum anchored heme-oxygenase 1 faces the cytosol. *Haematologica* **2012**, *97*, 1489. [[CrossRef](#)]
25. Chiang, S.-K.; Chen, S.-E.; Chang, L.-C. A dual role of heme oxygenase-1 in cancer cells. *Int. J. Mol. Sci.* **2018**, *20*, 39. [[CrossRef](#)] [[PubMed](#)]
26. Malfa, G.A.; Tomasello, B.; Acquaviva, R.; Genovese, C.; La Mantia, A.; Cammarata, F.P.; Ragusa, M.; Renis, M.; Di Giacomo, C. *Betula etnensis* Raf.(Betulaceae) extract induced HO-1 expression and ferroptosis cell death in human colon cancer cells. *Int. J. Mol. Sci.* **2019**, *20*, 2723. [[CrossRef](#)] [[PubMed](#)]
27. Kwon, M.-Y.; Park, E.; Lee, S.-J.; Chung, S.W. Heme oxygenase-1 accelerates erastin-induced ferroptotic cell death. *Oncotarget* **2015**, *6*, 24393. [[CrossRef](#)] [[PubMed](#)]
28. Chang, L.-C.; Chiang, S.-K.; Chen, S.-E.; Yu, Y.-L.; Chou, R.-H.; Chang, W.-C. Heme oxygenase-1 mediates BAY 11–7085 induced ferroptosis. *Cancer Lett.* **2018**, *416*, 124–137. [[CrossRef](#)]
29. Fang, X.; Wang, H.; Han, D.; Xie, E.; Yang, X.; Wei, J.; Gu, S.; Gao, F.; Zhu, N.; Yin, X. Ferroptosis as a target for protection against cardiomyopathy. *Proc. Natl. Acad. Sci. USA* **2019**, *116*, 2672–2680. [[CrossRef](#)] [[PubMed](#)]
30. Hassannia, B.; Wiernicki, B.; Ingold, I.; Qu, F.; Van Herck, S.; Tyurina, Y.Y.; Bayır, H.; Abhari, B.A.; Angeli, J.P.F.; Choi, S.M. Nano-targeted induction of dual ferroptotic mechanisms eradicates high-risk neuroblastoma. *J. Clin. Investig.* **2018**, *128*, 3341–3355. [[CrossRef](#)]
31. Zeeshan, H.M.A.; Lee, G.H.; Kim, H.-R.; Chae, H.-J. Endoplasmic reticulum stress and associated ROS. *Int. J. Mol. Sci.* **2016**, *17*, 327. [[CrossRef](#)]
32. Cao, S.S.; Kaufman, R.J. Endoplasmic reticulum stress and oxidative stress in cell fate decision and human disease. *Antioxid. Redox Signal.* **2014**, *21*, 396–413. [[CrossRef](#)]
33. Wang, M.; Kaufman, R.J. The impact of the endoplasmic reticulum protein-folding environment on cancer development. *Nat. Rev. Cancer* **2014**, *14*, 581–597. [[CrossRef](#)]
34. Qaisiya, M.; Zabetta, C.D.C.; Bellarosa, C.; Tiribelli, C. Bilirubin mediated oxidative stress involves antioxidant response activation via Nrf2 pathway. *Cell. Signal.* **2014**, *26*, 512–520. [[CrossRef](#)]
35. Sano, R.; Reed, J.C. ER stress-induced cell death mechanisms. *Biochim. Biophys. Acta (BBA)-Mol. Cell Res.* **2013**, *1833*, 3460–3470. [[CrossRef](#)] [[PubMed](#)]
36. Häcker, G. ER-stress and apoptosis: Molecular mechanisms and potential relevance in infection. *Microbes Infect.* **2014**, *16*, 805–810. [[CrossRef](#)] [[PubMed](#)]
37. Su, L.-J.; Zhang, J.-H.; Gomez, H.; Murugan, R.; Hong, X.; Xu, D.; Jiang, F.; Peng, Z.-Y. Reactive oxygen species-induced lipid peroxidation in apoptosis, autophagy, and ferroptosis. *Oxidative Med. Cell. Longev.* **2019**, *2019*, 5080843. [[CrossRef](#)] [[PubMed](#)]
38. Lee, Y.-S.; Lee, D.-H.; Choudry, H.A.; Bartlett, D.L.; Lee, Y.J. Ferroptosis-induced endoplasmic reticulum stress: Cross-talk between ferroptosis and apoptosis. *Mol. Cancer Res.* **2018**, *16*, 1073–1076. [[CrossRef](#)]
39. Lindskog, M.; Kogner, P.; Ponthan, F.; Schweinhardt, P.; Sandstedt, B.; Heiden, T.; Helms, G.; Spenger, C. Noninvasive estimation of tumour viability in a xenograft model of human neuroblastoma with proton magnetic resonance spectroscopy (1H MRS). *Br. J. Cancer* **2003**, *88*, 478–485. [[CrossRef](#)] [[PubMed](#)]
40. Tedeschi, G.; Lundbom, N.; Raman, R.; Bonavita, S.; Duyn, J.H.; Alger, J.R.; Di Chiro, G. Increased choline signal coinciding with malignant degeneration of cerebral gliomas: A serial proton magnetic resonance spectroscopy imaging study. *J. Neurosurg.* **1997**, *87*, 516–524. [[CrossRef](#)] [[PubMed](#)]